Glycobiology vol. 7 no. 3 pp. 337–347, 1997

Solution conformation of Lewis a–derived selectin ligands is unaffected by anionic substituents at the 3′- and 6′- positions

Josh W.Kurutz and Laura L.Kiessling[1,2]

Biophysics Program and [1]Department of Chemistry, University of Wisconsin–Madison, Madison, WI 53706, USA

[2]To whom correspondence should be addressed

The selectins are a family of proteins that mediate leukocyte tethering and rolling along the vascular endothelium. E-, P-, and L-selectin recognize various derivatives of the Lewis^a and Lewis^x trisaccharides. The distribution of negative charges on the Lewis^a and Lewis^x oligosaccharides appears to be an important factor in their binding by the selectins. Previous work exploring this electrostatic dependence found that a series of synthetic anionic trisaccharides, 3′-sulfo, 3′-phospho, 6′-sulfo, and 3′,6′-disulfo Lewis^a-(Glc), exhibited differing selectin inhibitory efficacies. To explore the possibility that these differences arise from conformational differences between the sugars, the solution structures of these trisaccharides were determined using NMR and molecular dynamics simulations. Interproton distances and interglycosidic torsion angles were determined at 37°C using NOESY buildup curves and 1D LRJ experiments, respectively. Data from both experiments agreed well with predictions made from 2000 picosecond unrestrained molecular dynamics simulations. We found that 3′-sulfation did not alter the core Lewis^a conformation, a finding that reaffirms the results of previous study. In addition, we found that sulfation at the 6′ position also leaves the trisaccharide conformation unperturbed. This is significant because the proximity of the 6′-sulfate group to the fucose ring might have altered the canonical Lewis^a structure. The disulfate exhibited greater flexibility than the other derivatives in dynamics simulations, but not so much as to affect NOE and heteronuclear coupling constant measurements. Taken together, our findings support the use of Lewis^a as a template onto which charged groups may be added without significantly altering the trisaccharide's structure.

Key words: oligosaccharides/molecular dynamics simulations/NMR/sulfated Lewis^a/phosphorylated Lewis^a

Introduction

Selectin-mediated adhesion of leukocytes to vascular endothelium is a critical element of the inflammatory immune response (Harlan and Liu, 1992). The carbohydrate ligands of the selectins have attracted a great deal of attention due to their importance to human physiology and their potential as leads for anti-inflammatory therapeutic agents (Harlan and Liu, 1992; Bevilacqua *et al.*, 1994; Rosen and Bertozzi, 1994; Varki, 1994; Kubes *et al.*, 1995; Lasky, 1995; McEver *et al.*, 1995). A number of selectin ligands and molecules that inhibit selectin-mediated adhesion have been identified (Nelson *et al.*, 1993; Varki, 1994; Kogan *et al.*, 1995; Manning *et al.*, 1995, 1996; Sanders *et al.*, 1996; Wu *et al.*, 1996), but the molecular basis of the selectin specificity has yet to be fully elucidated. Detailed knowledge about the carbohydrate ligands and their binding properties will be essential for a complete understanding of the biology of leukocyte adhesion and for the development of new approaches to drug design.

To clarify issues of selectin specificity and elucidate leads to high affinity selectin ligands, our laboratory is investigating the electrostatic character of selectin binding by synthesizing analogs of naturally occurring selectin ligands and correlating their charge distribution with inhibitory efficacy (Manning *et al.*, 1995, 1996; Sanders *et al.*, 1996). 3′-Sulfated Lewis a (Le^a) and 6′-sulfated sialyl Lewis x (sLe^x) have both been identified as naturally occurring selectin ligands (Yuen *et al.*, 1992, 1994; Hemmerich *et al.*, 1995), inspiring our synthesis of a series of anionic Le^a derivatives and the assessment of their inhibitory potencies (Figure 1).

Our anionic Le^a derivatives display a pattern of selectin inhibition that suggests that specifically located negative charges on the ligand are important factors in selectin discrimination, but they are not the sole determinants of affinity or specificity (Manning *et al.*, 1995, 1996; Sanders *et al.*, 1996). In an ELISA, 3′-sulfo Le^a(Glc) inhibits binding of P- and L-selectin to immobilized glycoprotein cell adhesion molecule-1 (GlyCAM-1), a mucin that interacts with all three selectins (Lasky *et al.*, 1992; Mebius and Watson, 1993; Hemmerich *et al.*, 1995; Diacovo *et al.*, 1996), with IC_{50} values similar to those found for 3′-sulfo Le^x and sLe^x (Manning *et al.*, 1995). In contrast, 3′-sulfo Le^a(Glc) is 20-fold more active against E-selectin than is 3′-sulfo Le^x. Placement of a phosphate group at the 3′ position on an Le^a template leads to a slight increase in affinity for E- and L-selectin relative to 3′-sulfo Le^a(Glc) (Manning *et al.*, 1996). The dianionic saccharide 6′-sulfo sLe^x has been shown to be a GlyCAM-1 determinant, and it displays all the features required for binding to L-selectin: sialylation, sulfation, and fucosylation (Hemmerich and Rosen, 1994; Hemmerich *et al.*, 1995; Maly *et al.*, 1996). However, compounds designed to mimic this determinant, 3′,6′-disulfo Le^a(Glc) and 3′,6′-disulfo Le^x(Glc), were no more effective than 3′-sulfo Le^x at blocking L-selectin binding to GlyCAM-1 (Manning *et al.*, 1995; Sanders *et al.*, 1996). Despite the observations that sulfated GlyCAM-1 binds L-selectin with high affinity and that sulfation of the 6′ position of galactose is a rare modification (Hemmerich *et al.*, 1995), a 6′-sulfo group when presented in concert with a 3′-sulfo substituent appears to contribute little to binding affinity (Sanders *et al.*, 1996).

Inhibition data for selectin ligands is expected to reflect anionic group distribution and/or charge density of the saccharide determinants, yet changes in sulfation patterns might alter saccharide ligand conformation, a result that could also account for changes in inhibitory potency. To begin to dissect the features responsible for changes in activity, the solution struc-

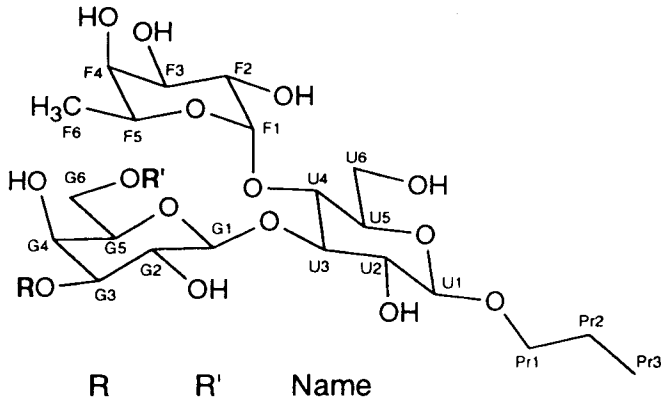

R	R'	Name
SO_3^-	H	3'-sulfo Le^a(Glc)
PO_3^{2-}	H	3'-phospho Le^a(Glc)
H	SO_3^-	6'-sulfo Le^a(Glc)
SO_3^-	SO_3^-	3',6'-disulfo Le^a(Glc)

Fig. 1. Synthetic selectin ligands and their numbering scheme.

tures of four anionic Le^a derivatives, 3'-sulfo Le^a (Glc), 3'-phospho Le^a (Glc), 6'-sulfo Le^a(Glc), 3',6'-disulfo Le^a (Glc), were determined by NMR and molecular modeling. Ring conformations were evaluated by measuring ^{1}H-^{1}H scalar coupling constants from the 1D spectra. Long-range J (LRJ) experiments were performed to estimate average interglycosidic torsion angles by measuring $^3J_{CH}$ values (Tvaroska *et al.*, 1989; Adams and Lerner, 1993). To measure ^{1}H-^{1}H distances, 2D NOESY experiments were conducted using several mixing times. These experimental results were compared to theoretical predictions derived from molecular dynamics simulations to afford insight into the conformational preferences of the trisaccharides.

Our data indicate that the Le^a(Glc) derivative core conformation is unperturbed by anionic substitution at the 3' and 6' positions. Such conformational homology between species of differing charge and charge placement suggests that sterics dominate the forces governing Le^a conformation. Significantly, our results suggest that differences in inhibitory potency between these compounds do not arise from differences in their conformations.

Table I. ^{1}H NMR chemical shifts at 37°C of anionic Le^a(Glc) derivatives, referenced to external TSP at –0.015 ppm (error = ± 0.0004 ppm)

Proton	3'-S Le^a(Glc)	3'-P Le^a(Glc)	6'-S Le^a(Glc)	3',6'-S Le^a(Glc)
Fuc1	4.982	4.957	4.952	4.978
Fuc2	3.781	3.753	3.738	3.764
Fuc3	3.880	3.858	3.877	3.916
Fuc4	3.786	3.759	3.782	3.810
Fuc5	4.840	4.825	4.839	4.873
Fuc6	1.180	1.159	1.165	1.193
Gal1	4.927	4.846	4.816	4.959
Gal2	3.673	3.630	3.533	3.698
Gal3	4.313	4.031	3.650	4.353
Gal4	4.262	4.054	3.932	4.315
Gal5	3.648	3.610	3.808	3.898
Gal6	3.737	3.710	4.150	4.195
Gal6'	3.737	3.708	4.109	4.145
Glc1	4.462	4.444	4.450	4.485
Glc2	3.519	3.482	3.476	3.519
Glc3	4.003	3.965	3.963	4.027
Glc4	3.671	3.640	3.626	3.660
Glc5	3.536	3.510	3.526	3.559
Glc6	3.964	3.926	3.950	3.981
Glc6'	3.810	3.783	3.803	3.833
Pr1	3.848	3.823	3.833	3.863
Pr1'	3.624	3.606	3.615	3.643
Pr2	1.617	1.590	1.598	1.630
Pr3	0.905	0.876	0.887	0.917

Table II. ^{1}H-^{1}H scalar coupling constants, in Hz, plus values predicted for chair forms using the algorithm of Altona and Haasnoot (error = ± 0.1 Hz)

Coupling constant	3'-S Le^a(Glc)	3'-P Le^a(Glc)	6'-S Le^a(Glc)	3',6'-S Le^a(Glc)	Theory
Fuc J1,2	4.0	4.0	4.0	4.0	3.6
Fuc J2,3	10.5	10.5	10.4	10.5	9.4
Fuc J3,4	3.3	3.3	3.3	3.3	3.1
Fuc J4,5	≤1.0	≤1.0	≤1.0	≤1.0	0.8
Fuc J5,6	6.6	6.6	6.6	6.6	N.D.
Gal J1,2	7.8	8.0	7.9	7.9	8.0
Gal J2,3	9.8	9.8	9.8	9.8	9.4
Gal J3,4	3.2	3.1	3.4	3.3	3.1
Gal J4,5	≤1.0	≤1.0	≤1.0	≤1.0	0.8
Gal J5,6	5.7	5.2	5.1	4.8	N.D.
Gal J5,6'	6.3	6.2	7.3	7.4	N.D.
Gal J6,6'	N.D.	N.D.	10.5	10.5	N.D.
Glc J1,2	8.0	8.1	8.1	8.0	8.0
Glc J2,3	9.3	9.2	9.2	9.2	9.4
Glc J3,4	9.3	9.4	9.2	9.2	9.4
Glc J4,5	9.7	9.8	9.6	9.8	8.0
Glc J5,6	2.1	2.1	2.0	2.1	N.D.
Glc J5,6'	4.6	4.5	4.7	4.4	N.D.
Glc J6,6'	12.3	12.4	12.3	12.3	N.D.
Pr J1,1'	10.0	9.9	9.9	9.9	N.D.
Pr J1,2	6.8	6.8	6.8	6.8	N.D.
Pr J1',2	6.8	6.8	6.8	6.8	N.D.
Pr J2,3	7.4	7.3	7.4	7.4	N.D.

Results and discussion

Assignment and strong coupling quantification

Assignment of ^{1}H and ^{13}C signals (Tables I–III) was accomplished using standard 1D and 2D techniques, as described in the Materials and methods section. Narrow linewidths (1.0–2.5 Hz) afforded precise determination of ^{1}H assignments and ^{1}H-^{1}H coupling constants from the 1D spectra. The effects of sulfation on chemical shifts are evident in the downfield shifts of the galactose 3' and 6' resonances relative to their nonsulfated counterparts.

The narrow spectral range characteristic of carbohydrate protons poses great overlap difficulties (Neuhaus and Williamson, 1989; van Halbeek, 1994) and makes them prone to appreciable strong coupling effects (Holmbeck *et al.*, 1994). These effects not only distort lines in the spectrum but can lead to incorrect interproton distance measurements due to changes in NOE intensities. Strong coupling parameters, S, were calculated for all four derivatives (Table IV) from the following equation (Neuhaus and Williamson, 1989):

$$S = \sin(\tan^{-1}(^3J_{HH}/\Delta\delta)) \quad (1)$$

When the parameter S is greater than approximately 0.1, line

Table III. ^{13}C chemical shifts at 37°C, referenced from the ^{1}H spectrum; quantities were measured from HMQC spectra (error = ± 0.1 ppm)

Carbon	3′-S Le^a(Glc)	3′-P Le^a(Glc)	6′-S Le^a(Glc)	3′,6′-S Le^a(Glc)
Fuc1	99.7	99.6	99.8	99.8
Fuc2	69.6	69.5	69.7	69.7
Fuc3	70.9	70.8	70.8	70.8
Fuc4	73.6	73.6	73.7	73.5
Fuc5	68.5	68.4	68.4	68.4
Fuc6	17.0	16.9	17.0	17.0
Gal1	103.9	104.0	104.3	103.9
Gal2	70.8	72.3	72.7	70.7
Gal3	82.1	78.1	74.2	81.8
Gal4	68.6	69.7	69.8	68.3
Gal5	76.1	76.2	73.9	73.7
Gal6	63.1	63.2	69.1	69.1
Glc1	103.8	103.7	103.6	103.7
Glc2	75.9	75.8	75.9	76.0
Glc3	80.7	80.7	81.2	81.2
Glc4	73.7	73.6	74.0	73.9
Glc5	77.1	77.0	77.1	77.1
Glc6	61.5	61.4	61.5	61.5
Pr1	74.0	74.0	73.9	73.9
Pr2	23.8	23.7	23.7	23.7
Pr3	11.2	11.2	11.2	11.2

intensities within a multiplet are noticeably affected. When S is greater than approximately 0.2, kinetic NOE measurements are influenced. Four proton pairs exhibited significant strong coupling in all compounds: Fuc2/3, Gal4/5, Gal6/6′, and Glc6/6′. Gal6/6′ was so strongly coupled that no structural information could be obtained from their analysis, though this data would have been useful for describing the conformational preference of this hydroxymethyl group. Strong coupling between GlcH6 and GlcH6′ was moderate, giving rise to distortion of line intensities but negligible effects on the NOE intensity.

Ring conformations

Theoretical predictions of $^{3}J_{HH}$ for idealized chair conformations of α-L-fucose, β-D-galactose, and β-D-glucose were computed (Altona and Haasnoot, 1980) and are presented in Table II alongside the corresponding experimental values. The predicted and measured $^{3}J_{HH}$ values were very close in almost all cases, suggesting that the glucose and galactose rings are in $^{4}C_1$ conformation and fucose is in $^{1}C_4$ (Stoddart, 1971). The two coupling constants that diverge by more than 1.0 Hz from those predicted by theory are Fuc J2,3 and Glc J4,5, both of which are strongly coupled (see Table IV). Therefore, these quantities are not likely to accurately reflect ring conformation.

Table IV. Significant strong coupling parameters, S, calculated using Equation 1

Coupling	3′-S Le^a(Glc)	3′-P Le^a(Glc)	6′-S Le^a(Glc)	3′,6′-S Le^a(Glc)
Fuc 2,3	0.21	0.20	0.15	0.14
Gal 2,3	0.03	0.05	0.17	0.03
Gal 3,4	0.13	0.26	0.02	0.17
Gal 5,6	0.13	0.10	0.03	0.03
Gal 5,6′	0.14	0.13	0.05	0.06
Gal 6,6′	~1.0	~1.0	0.46	0.39
Glc 4,5	0.14	0.15	0.19	0.19
Glc 6,6′	0.16	0.16	0.17	0.16

When S is greater than approximately 0.2, distortions of NOESY peak intensities involving either member of the pair will be significant.

Table V. Φ (H1-C1-O1-Ca) and Ψ (C1-O1-Ca-Ha) dihedral angles

	3′-S Le^a(Glc)	3′-P Le^a(Glc)	6′-S Le^a(Glc)	3′,6′-S Le^a(Glc)
Fuc-Ψ-Glc				
Model	19	19	19	19
$^{3}J_{CH}$	5.2 ± 0.4 Hz	4.8 ± 0.4	5.4 ± 0.5	4.8 ± 0.4
Experiment	16	23	11	23
Lower limit	0	16	0	16
Upper limit	23	28	21	28
Gal-Ψ-Glc				
Model	20	21	20	19
$^{3}J_{CH}$	5.1 ± 0.4 Hz	4.7 ± 0.4	5.1 ± 0.5	4.7 ± 0.4
Experiment	18	24	18	24
Lower Limit	8	18	0	18
Upper limit	24	29	26	29
Fuc-Φ-Glc				
Model	46	47	47	47
Experiment	N.D.	N.D.	N.D.	N.D.
Lower limit	44	44	44	44
Upper limit	128	128	128	128
Gal-Φ-Glc				
Model	46	46	45	46
Experiment	N.D.	N.D.	N.D.	N.D.
Lower limit	44	44	44	44
Upper limit	128	128	128	128

Experimental torsions were calculated from measured $^{3}J_{CH}$ values using the Karplus relation of Tvaroska (Tvaroska, 1989). Maximum and minimum average angles were estimated based on the error in determining $^{3}J_{CH}$. N.D., Not determined.

Interglycosidic torsion angles

LRJ experiments (Adams and Lerner, 1993) were employed to measure three-bond carbon-hydrogen scalar couplings, $^{3}J_{CH}$,

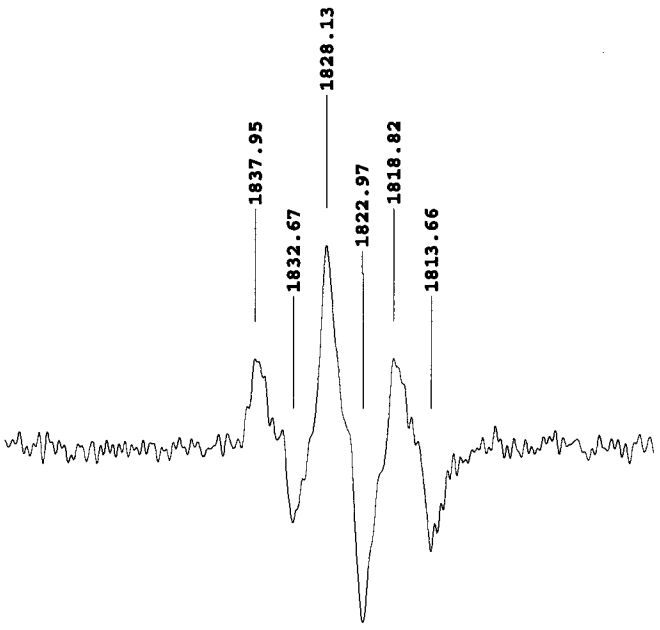

Fig. 2. The GlcH4 resonance of 3′-phospho Le^a(Glc) observed in the 1D LRJ experiment. Antiphase splitting indicates coupling to the anomeric carbon of fucose. The spectrum is the sum of 8192 transients, and was multiplied by a gaussian window function to reduce noise.

which are related to interglycosidic torsion angles (Tvaroska *et al.*, 1989) (Table V). In the LRJ experiments, proton lines retain $^3J_{HH}$ in-phase splittings, but are modified by antiphase splitting of $^3J_{CH}$. $^3J_{CH}$ is then reckoned as the frequency difference between positive and negative peaks. (Figure 2) This measurement is subject to error due to cancellation of positive and negative peaks when $^3J_{CH}$ is approximately equal to $^3J_{HH}$ and/or when $^3J_{CH}$ is approximately equal to the peak linewidth. Such error became significant in determinations of interglycosidic Φ angles, as discussed below.

Ranges of acceptable average torsions were determined from the estimated error in measurement of $^3J_{CH}$. Because each value of J below 5.6 Hz corresponds to four possible torsion angles in this Karplus curve, the angles reported were restricted to the only set consistent with NOE data. The $^3J_{CH}$ values corresponding to Ψ angles were readily measured by 1D LRJ experiments as the anomeric ^{13}C and ^1H resonances were well resolved and gave rise to coupling constants of approximately 5 Hz. In this region of the Karplus curve, small changes in J yield large changes in Ψ angles, a relationship that is reflected in the large range of acceptable average torsion angles that the measured couplings might represent. The Φ angles could not be determined precisely because significant crosspeaks in the 2D LRJ spectra could not be detected. It is likely that the $^3J_{CH}$ values corresponding to Φ angles were small enough ($^3J_{CH} \sim \Delta\nu_{1/2}$) that cancellation between positive and negative peaks reduced the signal intensity dramatically. If $^3J_{CH}$ approximately equaled $^3J_{HH}$, the center peaks would have canceled, but outer peaks would have remained. Thus, the absence of observable coupling suggests that $^3J_{CH}$ was less than approximately 3 Hz, which restricts the average Φ angles to the range $44° \leq \Phi \leq 128°$. This range is consistent with theoretical predictions based on molecular dynamics simulations.

NOESY

2D NOESY (Jeener *et al.*, 1979; Macura *et al.*, 1981; Neuhaus and Williamson, 1989; Cavanagh *et al.*, 1996) data were acquired at 37°C to enable facile detection and reliable quantitation of crosspeak volumes (Figure 3). Temperature had a significant effect on the magnitude and sign of the NOE intensities, as expected for molecules in this molecular weight range. Overall NOE intensity was negligible at ambient temperature and was negative at 2°C. Experiments detecting positive NOEs at 37°C were conducted to avoid the line broadening experienced by these samples at lower temperatures. 1D ^1H experiments, performed on all compounds between 2°C and 42°C, revealed that chemical shifts and ^1H-^1H coupling constants were not significantly temperature-dependent, suggest-

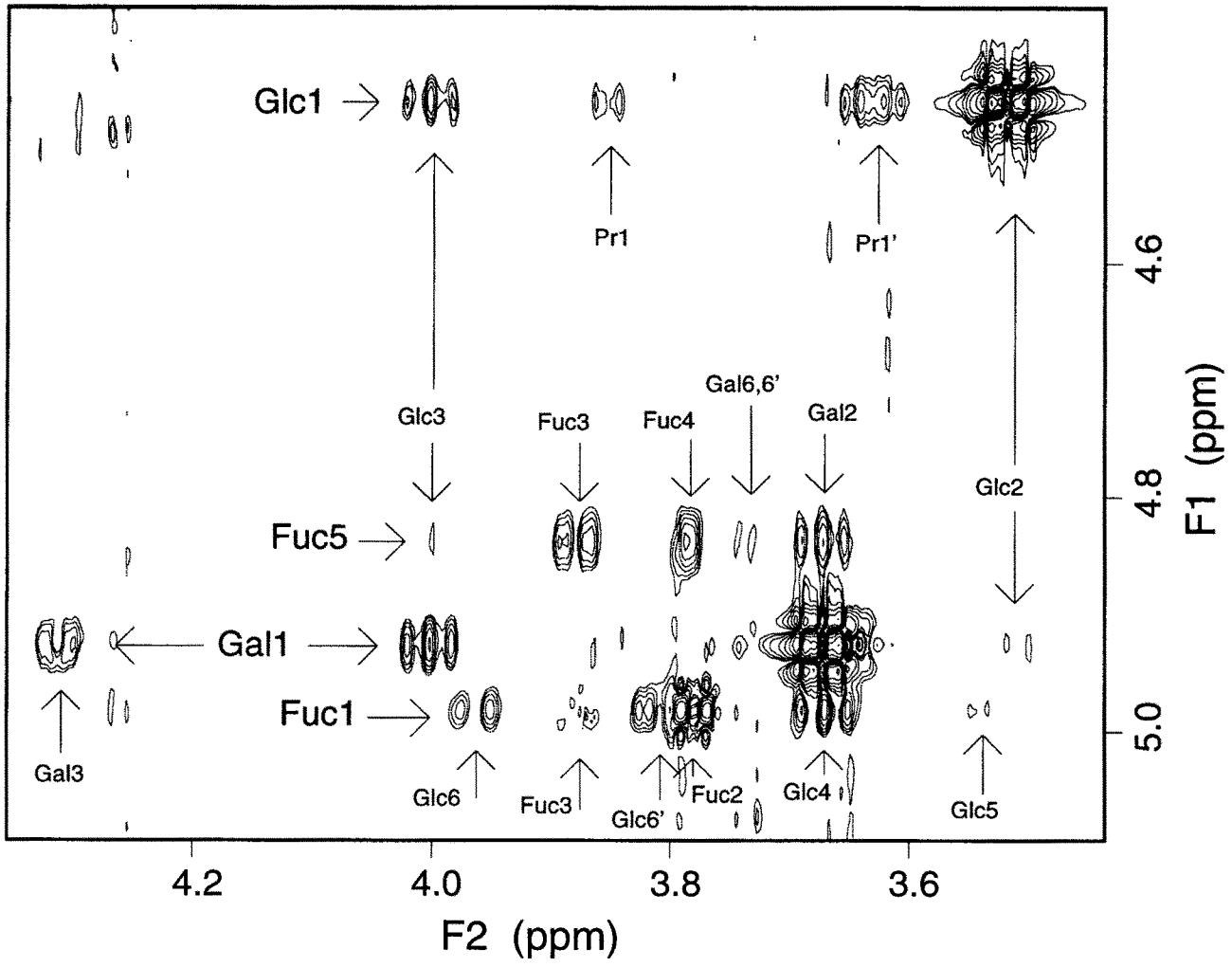

Fig. 3. Portion of 3'-sulfo Le^a(Glc) NOESY spectrum, acquired with a 300 ms mixing time, representing contacts between anomeric and Fuc5 hydrogens (F1 dimension) with ring and methylene signals (F2 dimension).

ing that data acquired at the elevated temperature accurately reports on the conformation and dynamics of the trisaccharides over the temperature range studied.

Although the NOE intensities at 37°C were smaller than those detected by ROESY experiments performed at the same temperature (data not shown), NOESY experiments were chosen for this study. ROESY data (Bothner-By *et al.*, 1984) is complicated by Hartmann-Hahn effects (TOCSY), laboratory frame dipolar relaxation (NOESY), and a dependence of the cross-relaxation rate on offset from the spin lock frequency (Bax, 1988; Schleucher *et al.*, 1995). By finding conditions that afforded suitable NOE intensities, the difficulties of analyzing ROESY data were circumvented.

Although the integration of most peaks was straightforward, many valuable peaks were partially overlapped. In such cases, the resolved fraction of the peak was integrated and the total volume of the peak was extrapolated from that value using knowledge of the fractional intensity of that line in the multiplet. Distances calculated from crosspeaks measured this way are identified in Table VI. No corrections for intensity distortions arising from strong coupling were applied when using this method.

Crosspeak volumes were normalized to that of the downfield diagonal peak or, if possible, to the geometric mean of both diagonal peak volumes. For 6′-sulfo Le^a(Glc) and 3′-phospho Le^a(Glc), FucH5 and GalH1 signals were overlapped, and the diagonal peak intensities for each were approximated as half the combined diagonal peak intensity. The signals due to FucH1 and GalH1 were overlapped in the 3′,6′-disulfo Le^a-(Glc) spectrum, and their intensities were also evaluated as half of the combined diagonal peak volume.

NOESY experiments were performed using a number of different mixing times for each compound to directly observe buildup of transferred magnetization (Cavanagh *et al.*, 1996). Hydrogen T_1 values ranged from 0.5 to 2.0 s, so normalized NOE buildup was assumed to be linear over the range of mixing times used in these experiments (50–300 ms; Neuhaus and Williamson, 1989). To illustrate the application of this methods, NOE buildup curves for selected interglycosidic and reference NOEs are presented in Figure 4. The lines shown represent fitted curves, the slopes of which were taken to be the NOE cross relaxation rates representing interproton distances (Neuhaus and Williamson, 1989).

Distance calculations

Interproton distances (Table VI) were calculated from cross relaxation rates using the isolated spin pair approximation and the equation (Neuhaus and Williamson, 1989):

$$r_{ab} = r_{reference}\,(\sigma_{reference}/\sigma_{ab})^{1/6} \quad (2)$$

The reference NOE, $\sigma_{reference}$, used for measuring distances between ring and hydroxymethyl protons was that of the well-resolved GlcH1-H3 crosspeak for 3′-sulfo, 3′,6′-disulfo Le^a-(Glc), and 3′-phospho Le^a(Glc); 6′-sulfo Le^a(Glc) distances were referenced to the GalH1-H3 crosspeak. Theoretical distances, $r_{ab,theory}$, were calculated using the equation (Neuhaus and Williamson, 1989):

$$r_{ab,theory} = 1/((<1/r_{ab,i}{}^6>)^{1/6}) \quad (3)$$

where $r_{ab,i}$ are the instantaneous distances between protons A and B in the molecular dynamics simulation. The ⅙-root averaging method was chosen for most proton pairs instead of the ⅓-root averaging suggested by Tropp *et al.* (Tropp, 1980). The latter protocol applies to systems whose internal motions are fast relative to overall tumbling; but the potential "internal" motions here require relative displacements of ⅔ of the molecule, and it is unlikely that such movements will be fast. The ⅓-root method was used to calculate average distances from

Table VI. Comparison of experimentally- and theoretically-derived ^{1}H-^{1}H distances

Crosspeak	3′-S Le^a(Glc)		3′-P Le^a(Glc)		6′-S Le^a(Glc)		3′,6′-S Le^a(Glc)	
	NOE distance	Dynamically averaged distance	NOE distance	Dynamically averaged distance	NOE distance	Dynamically averaged distance	NOE distance	Dynamically averaged distance
Interglycosidic								
Fuc1/Glc4	2.19[b]	2.40	2.20	2.40	2.33	2.40	2.23[b,c]	2.41
Fuc1/Glc5	3.28[c]	3.78	3.40[c]	3.77	3.41	3.77	N.D.	3.76
Fuc1/Glc6	2.25[b,c]	2.51	2.47	2.50	2.61	2.49	2.73[c]	2.49
Fuc1/Glc6′	2.39	2.34	2.26[b]	2.35	2.44	2.33	2.41[c]	2.33
Gal1/Glc2	3.16[c]	3.65	2.96[c]	3.64	3.67[b]	3.66	3.44[c]	3.68
Gal2/Glc3	2.22[c]	2.40	2.16[c]	2.41	2.31[c]	2.38	2.38[c]	2.38
Gal2/Fuc5	2.19	2.59	O/L	2.59	O/L	2.62	2.49[c]	2.59
Gal2/Fuc6	2.93	3.15	3.01[c]	3.19	2.88[c]	3.26	2.95[c]	3.21
Intraglycosidic								
Glc1/Glc3	2.51[a]	2.51	2.51[a]	2.51	2.80	2.50	2.78[c]	2.50
Glc1/Glc5	O/L	2.39	O/L	2.33	2.41[b]	2.39	N.D.	2.39
Gal1/Gal3	2.44	2.56	O/L	2.58	2.42[c]	2.57	2.56[c]	2.56
Gal1/Gal5	O/L	2.32	O/L	2.33	2.31[a,c]	2.31	2.31[a,c]	2.31
Fuc4/Fuc6	3.00[a]	3.00	3.00[a]	3.02[a]	3.02[a]	3.02	3.01[a]	3.01

Modeled distances were derived by averaging over distances measured during molecular dynamics simulations using Equation 3. Experimentally determined distances were calculated from NOE buildup rates relative to the indicated reference interproton distances using Equation 2.

[a]Reference NOE distance.

[b]Distances measured from integrations of resolved fractions of partially overlapped NOE crosspeaks; volumes of total crosspeaks were extrapolated from these partial quantities.

[c]Distances calculated from crosspeaks normalized to an averaged value of two overlapped diagonal peaks.

O/L, Not determined due to overlap.

N.D., Not determined.

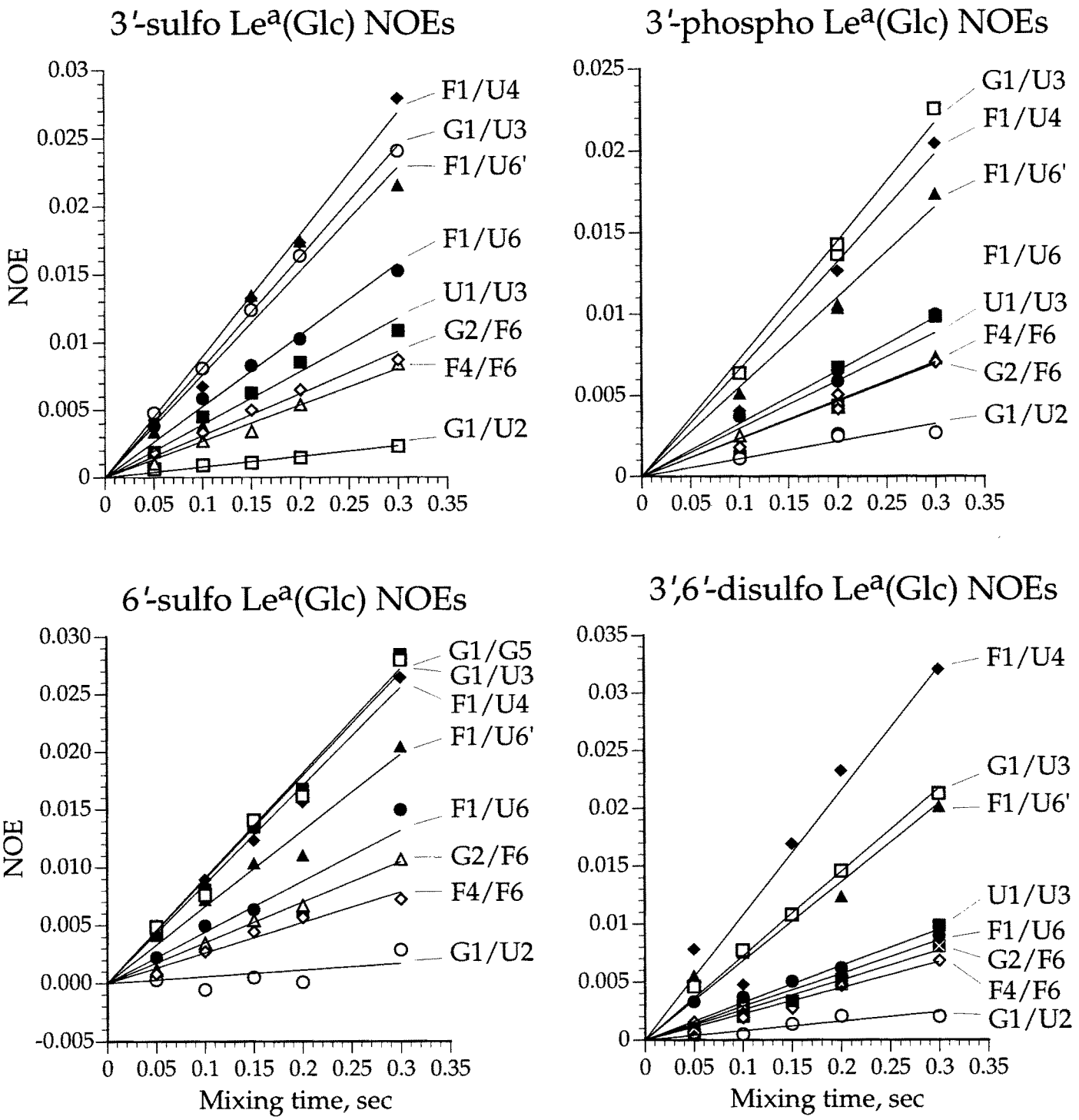

Fig. 4. NOE buildup curves for principal interglycosidic and reference contacts. Magnitudes reflect normalized crosspeak intensities.

the three FucH6 methyl protons (Neuahus and Williamson, 1989); the averaged distance between the methyl protons and FucH4 was used as the reference separation, $r_{reference}$.

Modeling

The model data, acquired using the MacroModel program with an all-atom AMBER* force field (Senderowitz *et al.*, 1996), suggest that these trisaccharides generally adopt single conformations but can travel far from their minimum in conformational space without significant energetic cost. Thus, the molecules appear to reside in a single broad potential well. This result agrees well with results observed previously for 3′-sulfo Le^a and related sugars (Bechtel *et al.*, 1990; Cagas and Bush, 1990; Mukhopadhyay and Bush, 1991; Ball *et al.*, 1992; Ichikawa *et al.*, 1992; Lin *et al.*, 1992; Miller *et al.*, 1992; Kogelberg and Rutherford, 1994; Mukhopadhyay *et al.*, 1994; Rutherford *et al.*, 1994; Coteron *et al.*, 1995; Kogelberg *et al.*, 1996).

Simulated annealing

All trisaccharides minimized readily to single conformations in the simulated annealing routines (Figure 5). Annealing was especially important for the 6′-sulfo Le^a(Glc) model. The initial conformation minimized by the PRCG (Polak Ribiere conjugate gradient) method (Polak and Ribiere, 1969), which placed the hydroxymethyl oxygen gauche to the ring oxygen, changed irreversibly to the trans form after approximately 100 ps of 37°C dynamics during the annealing treatment. Had the initial structure used for dynamics been obtained with only steepest-descent minimization (SD) instead of simulated annealing, the higher energy trans conformation would have been present in the subsequent dynamics simulation for 100 ps instead of 0.

A hydrogen bond, which is likely an artifact, was observed in the annealed structure of 3′-sulfo Le^a(Glc). In the annealed and energy-minimized structure, the glucose hydroxymethyl oxygen occupied a trans orientation relative to the ring oxygen in order to form a hydrogen bond to the fucose hydroxyl group at position 2. In contrast, NOE data indicate that the two oxygens are gauche, a preference predicted by electronic effects, and consistent with the measurements of the three other Le^a-(Glc) derivatives. Interestingly, this hydrogen bond is broken and a more realistic conformation is adopted after about 200 ps of molecular dynamics simulation. It is possible that the artifact derives from the use of a united-atom AMBER* force field rather than an all-atom force field (Senderowitz and Still, 1997).

Dynamics

All four derivatives exhibit single core conformations during the 2 nanoseconds of dynamics simulation (Figures 6 and 7). This result agrees with previous work on sLe^x, in which the trisaccharide core of the tetrasaccharide was found to be conformationally stable during 5 ns of molecular dynamics (Rutherford *et al.,* 1994). Thus, multiple stable interglycosidic orientations are unlikely to contribute to the monosulfated systems.

In our computational models, the galactose–glucose linkage appears slightly more conformationally flexible than the fucose–glucose linkage in these simulations. This result is interesting because some potential indicators of relative dynamic behavior, such as the difference between anomeric proton linewidths of fucose and galactose suggested that the fucose linkage might be more flexible (Ernst *et al.,* 1988; Cavanagh *et al.,* 1996). The experiments reported here, however, are not sufficiently sensitive to measure the differences in dynamic behavior between the linkages. Our computer simulation findings contrast with those of Rutherford *et al.,* who found the Gal-Ψ-Glc and Fuc-Ψ-Glc angles in sLe^x to be equally mobile in restrained dynamics simulations using an earlier version of the AMBER force field (Rutherford *et al.,* 1994). The source of these differences might lie in several factors that differed between the studies. The results may be attributed to the new modifications to the force field (Senderowitz *et al.,* 1996), the application of restraints in the previous simulation, or the differences between a sialyl and sulfo substituent on the galactose ring.

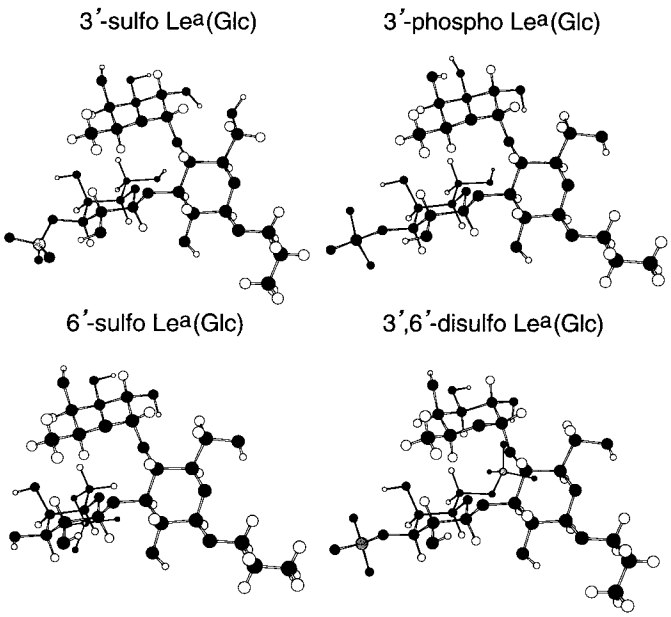

Fig. 5. Models of synthetic Le^a derivatives after simulated annealing.

Full conformational searching

To probe the likelihood of alternative conformations more rigorously, an extensive mixed mode Monte Carlo/stochastic dynamics (MCSD) routine with an all-atom force field parameterized for carbohydrates was applied to 6′-sulfo Le^a(Glc) and 3′,6′-disulfo Le^a(Glc), using a protocol developed by Still and coworkers (Senderowitz and Still, 1997). Again, no alternative conformations were found and the average distances and torsion angles predicted by MCSD generally agreed to within 0.1 Å and 3°, respectively, of the values derived using conventional dynamics (data not shown).

In this study, all computational modeling was performed without restraints derived from experiment. This was done for several reasons. First, it was not necessary to impose restraints for the model to agree with experiment. Second, acceptable ranges of torsion angles and distances used as constraints in modeling cannot be determined from the experiments performed. The data yield average distances and dihedral angles, but do not describe the amplitudes of their deviations in the molecule. For example, in our model of torsional motion, the galactose linkage is predicted to be more flexible than the fucose linkage. Their average theoretical interglycosidic dihedral angles, however, are nearly the same. This difference in amplitudes would not be detectable in the NMR experiments performed; consequently, any restraint placed on their motion in the computational model would have been arbitrary. Third, the few instances of disagreement between theory and experiment can reveal deficiencies in the theory only if the two are kept independent. For example, we detected a hydrogen bond in 3′-sulfo Le^a(Glc) that is probably an artifact of the modeling force field. Because the model was not restrained, unrealistic features of the force field, such as an overemphasis on hydrogen bonding, can be identified and corrected.

Implications for biological study

Our results support the use of the Le^a(Glc) trisaccharide as a conformationally invariant template to probe selectin binding. The 3′-sulfo Le^a(Glc) structure presented here concurs with one previously determined for 3′-sulfo Le^a by Kogelberg *et al.* (Kogelberg and Rutherford, 1994), suggesting that the *N*-acetyl substituent of Le^a does not significantly influence the core trisaccharide structure. Because sulfation at the 3′ and 6′ positions does not affect the interglycosidic orientations found in Le^a(Glc), we conclude that the solution structure of the Le^a

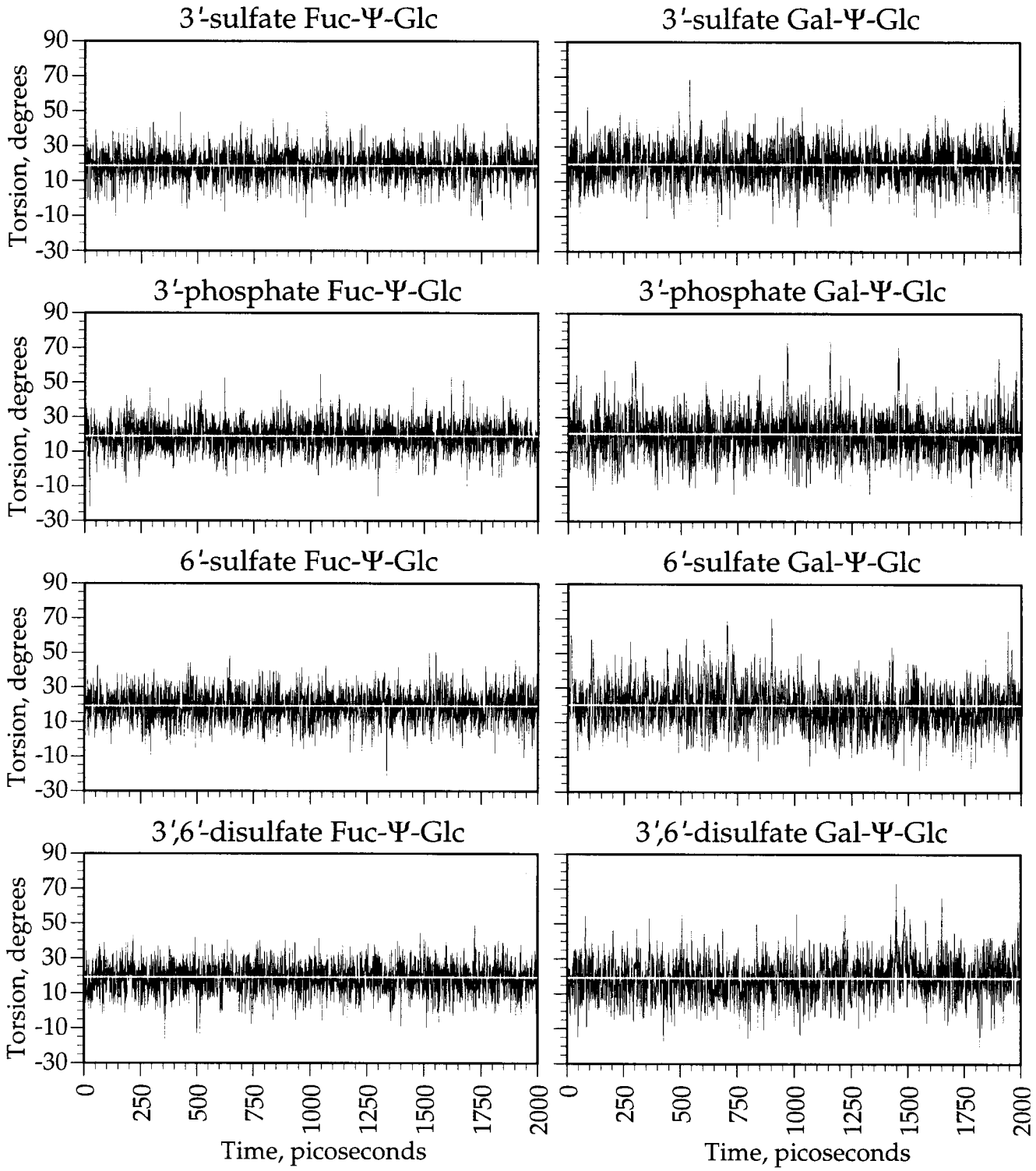

Fig. 6. Trajectories representing the time courses of interglycosidic Ψ torsions of the sulfated Le^a derivatives during 37°C molecular dynamics simulations. Horizontal white lines represent average angles.

core is unperturbed by modification at these biologically relevant sites.

The finding that sulfation, especially at the 6′ position, does not affect the Le^a core structure is significant. Previous studies have demonstrated that 3′-sulfation and sialylation do not modify the conformation of Le^a trisaccharide (Kogelberg and Rutherford, 1994; Rutherford *et al.*, 1994; Kogelberg *et al.*, 1996), but this is the first description of the effects of charged substitution at the 6′ position. 6′-Sulfation might have modified the relative orientations of the fucose and galactose rings due to the steric interactions, sulfate-fucose hydrogen bonding, or disruption of the solvent structure (Cantor and Schimmel, 1980; Lemieux, 1996) around the galactose hydroxymethyl group. Since these factors ultimately did not affect the trisac-

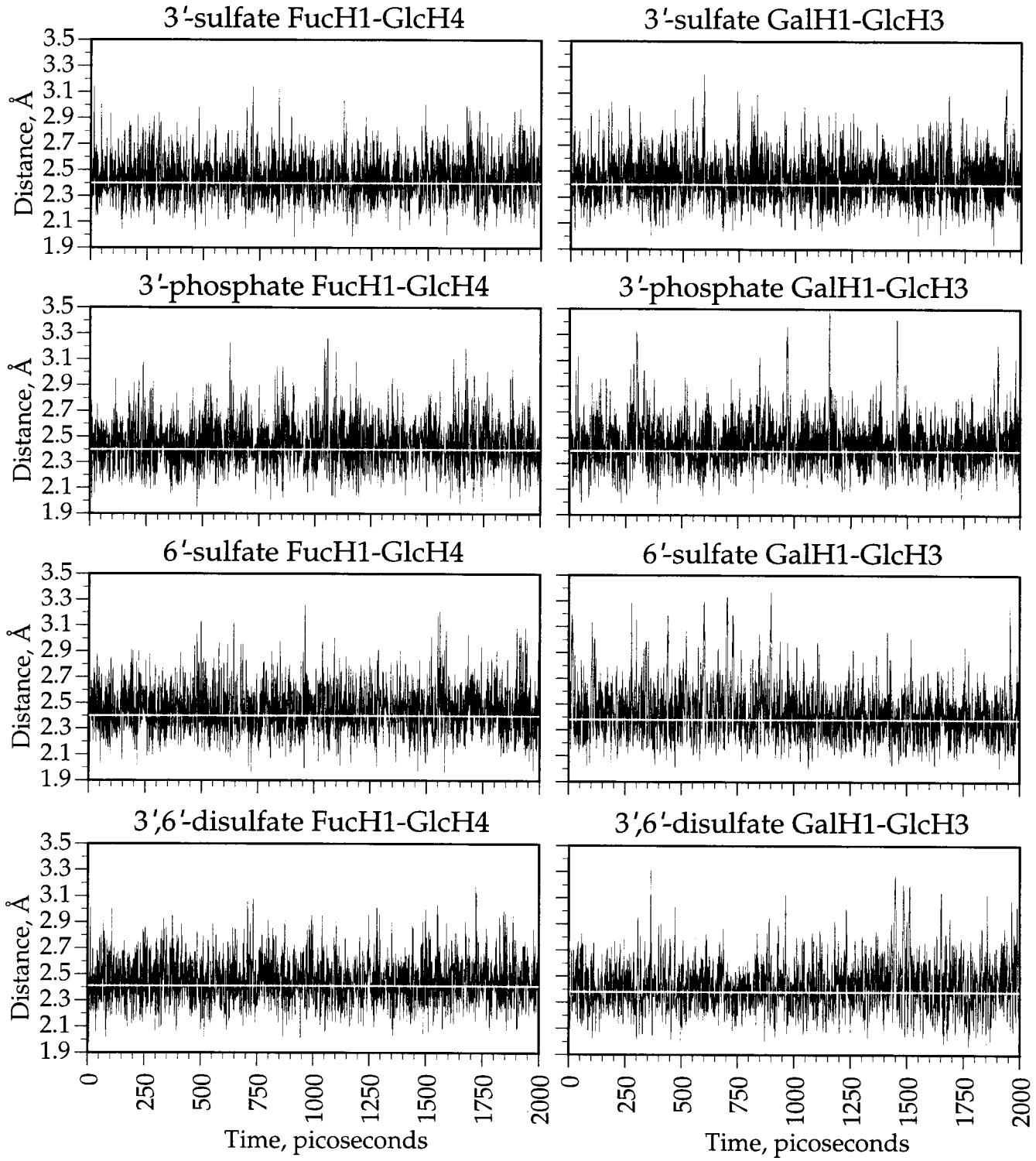

Fig. 7. Trajectories representing the time courses of FucH1-GlcH4 and GalH1-GlcH3 distances during 37°C molecular dynamics simulations. Horizontal white lines represent dynamically averaged distances calculated using Equation 3.

charide structure, we conclude that steric interactions between the galactose and fucose residues dominate the forces that determine Le^a conformation.

Materials and methods

Sample preparation

The sodium salt of each compound was dissolved in D_2O (99.9% D, Cambridge Isotope Labs), then the pH of the solutions were each adjusted to 7.0 ± 0.1 with mono- and dibasic sodium phosphate (99.95%, Aldrich). NaN_3 (0.05 mg, 99%; Aldrich) was added to prevent bacterial growth. After filtration through 0.1 μm Anotop syringe filters (Whatman), solutions were repeatedly frozen, sublimated using a Savant Speed-Vac, and redissolved with D_2O to exchange residual HDO for D_2O. The final sample dissolution employed highly isotopically enriched D_2O (0.25 ml, 99.996% D; Cambridge Isotope Labs), making 45 mM, 86 mM, and 24 mM solutions of 3′-sulfo, 6′-sulfo, and 3′,6′-disulfo Le^a(Glc) derivatives, respectively. 3′-phospho Le^a(Glc) was dissolved in 0.70 ml D_2O to yield a final concentration of 28 mM in a Wilmad 535-PP 5 mm NMR tube. Solutions of the other saccharides were transferred to Wilmad 327-PP 3 mm

NMR tubes; all were degassed under aspiration with sonication, and flushed with nitrogen.

Spectroscopy

All NMR spectroscopy reported was performed on a Varian VXR/Unity 500 MHz instrument equipped with a Nalorac Z-spec 3 mm triple resonance inverse detection probe; 3-phospho Le^a(Glc) in the 5 mm tube was analyzed using a 5 mm triple resonance inverse detection probe from Varian. For the variable temperature experiments described below, 3 mm carbohydrate sample tubes were inserted into 5 mm NMR tubes containing a TSP (sodium 3-trimethylsilylpropionate, d_4, 98% D, Cambridge Isotope Labs) reference solution; these samples were analyzed using the Varian 5 mm triple resonance probe.

Assignment of ^1H and ^{13}C resonances at 37°C was accomplished using a combination of DQCOSY, TOCSY, and HMQC techniques (Cavanagh *et al.*, 1996). In addition, assignments were made for protons at temperatures ranging from 2°C to 42°C; analysis of 1D spectra taken at different temperatures enabled assignment of several resonances of otherwise ambiguous identity.

NOESY

^1H-^1H distances in all four carbohydrates were measured at 37°C using 2D NOESY (Cavanagh *et al.*, 1996; Jeener *et al.*, 1979, Macura, 1980; Neuhaus and Williamson, 1989). Spectra were acquired at various mixing times, ranging from 50 to 300 ms. Mixing times for the 6′-sulfo Le^a derivative were randomized by 5% to reduce the magnitudes of the zero quantum coherence artifacts (Jeener *et al.*, 1979; Macura, 1981; Neuhaus and Williamson, 1989). A total of 2048 *t2* and 256 *t1* complex points were acquired for each spectrum; each *t1* increment was a composition of eight transients. Free induction decays were zero-filled to yield 2048 × 2048 point spectra.

$^3J_{CH}$ measurement

Interglycosidic three-bond CH coupling constants were measured using 1D and 2D LRJ experiments. ^{13}C pulse widths were calibrated by using a 90°(^1H) – tau(1/4 * $^1J_{CH}$) – 90°(^{13}C) – acq(^1H) sequence with an aqueous 2–^{13}C-NaOAc sample. When performing 1D LRJ experiments, short (<100 *t1* increments) HMQC experiments were performed to determine frequencies of carbon resonances needed for selective irradiation. The refocusing delays in the 1D experiments were set assuming 16 Hz or 8 Hz coupling constants to minimize relaxation effects while still achieving adequate refocusing. 1D experiments used between 2048 and 8192 transients. 2D experiments employed 2048 *t2* points and 256 *t1* points, and typically used 32–128 transients per *t1* increment.

Analysis

Spectra used for assignment and $^3J_{CH}$ measurement were processed using VNMR software by Varian. NOESY spectra were processed and crosspeaks integrated using Felix 3.2 (Biosym). Normalized crosspeak volumes were plotted against mixing time and fit to the equation y = mx. The resulting slopes, m, were treated as the NOE buildup rates and used to calculate average interproton distances.

Modeling

Molecular modeling was performed using MacroModel 5.0 on a Silicon Graphics Indy2 workstation. All procedures employed the GB/SA continuous dielectric aqueous solvation model (Still *et al.*, 1990) and the AMBER* force field equipped with carbohydrate-specific parameters (Homans, 1990; Senderowitz *et al.*, 1996).

Geometries of input structures were optimized using a steepest-descent algorithm, followed by a round of PRCG energy minimization (Polak and Ribiere, 1969). Unrestrained simulated annealing was performed by placing these structures in a 37°C dynamics bath for 150 ps, cooling them in 1.0 fs timesteps to –118°C over 150 ps, allowing them to explore conformations at –273°C for 10 ps, and then optimizing their geometries using PRCG energy minimization. These minimized structures are the sources of the depictions used in this report (Figure 5).

Molecular dynamics at 37°C were performed for a theoretical prediction of the full range of conformers accessible to the compounds of interest. Compounds in their annealed conformations were placed in a 37°C bath for 2000 ps, with a temperature bath update period of 0.2 ps; the timestep increment along the trajectory was 1.0 fs, and structures were sampled once every picosecond, resulting in 2000 structures per compound per trajectory.

Acknowledgments

This research was supported by grants from the NIH (GM-49975) and NSF (NYI Award to L.L.K). L.L.K. acknowledges the American Cancer Society, the Beckman Foundation, the Camille and Henry Dreyfus Foundation, and the Milwaukee Foundation for support. J.W.K. was supported by the Biophysics Training Program (T32-GM08293–05).

Abbreviations

sLe^x, sialyl Lewis x; Le^x, Lewis x; Le^a, Lewis^a; Le^a(Glc), galactose-β1→3(fucoseα1→4)glucoseβ-O-propyl; Fuc, fucose; Glc, glucose; Gal, galactose; Sug, sugar; Fuc*HN*, where *N* = 1→6,6′, hydrogen at position number N on fucose—similar for Gal*HN* and Glc*HN*; GlcH6/GalH6, downfield hydrogen at glucose/galactose position 6; GlcH6′/GalH6′, upfield hydrogen at glucose/galactose position 6; Sug*HN*/Sug*HN*′, designation for crosspeak between Sug*HN* (F1 dimension) and Sug*HN*′ (F2 dimension); ELISA, enzyme-linked immunosorbent assay; GlyCAM-1, glycoprotein cell adhesion molecule-1; Φ, interglycosidic dihedral defined by H1-C1-O1-Cx, where x represents aglyconic atoms; Ψ, interglycosidic dihedral defined by C1-O1-Cx-Hx; LRJ, long range J experiment; NOESY, nuclear Overhauser effect spectroscopy; DQCOSY, double quantum filtered correlated spectroscopy; TOCSY, total correlation spectroscopy; HMQC, heteronuclear multiple quantum coherence spectroscopy; SD, steepest descent; PRCG, Polak Ribiere conjugate gradient.

References

Adams,B. and Lerner,L. (1993) Measurement of long-range 1H-13C coupling constants using selective excitation of carbon-13. *J. Mag. Res., Ser. A,* **103,** 97–102.

Altona,C. and Haasnoot,C.A.G. (1980) Prediction of anti and gauche vicinal proton-proton coupling constants in carbohydrates: a simple additivity rule for pyranose rings. *Org. Mag. Res.,* **13,** 417–419.

Ball,G.E., O'Neill,R.A., Schultz,J.E., Lowe,J.B., Weston,B.W., Nagy,J.O., Brown,J.B., Hobbs,C.J. and Bednarski,M.D. (1992) Synthesis and structural Analysis using 2-D NMR of sialyl Lewis x (SLex) and Lewis x (Lex) oligosaccharides: ligands related to E-selectin [ELAM-1] binding. *J. Am. Chem. Soc.,* **114,** 5449–5451.

Bax,A. (1988) Correction of cross-peak intensities in 2D spin-locked NOE spectroscopy for offset and Hartmann-Hahn effects. *J. Mag. Res.,* **77,** 134–147.

Bechtel,B., Wand,A.J., Wroblewski,K., Koprowski,H. and Thurin,J. (1990) Conformational analysis of the tumor-associated carbohydrate antigen 19–9 and its Le^a blood group antigen component as related to the specificity of monclonal antibody CO19–9. *J. Biol. Chem.,* **265,** 2028–2037.

Bevilacqua,M.P., Nelson,R.M., Mannori,G. and Cecconi,O. (1994) Endothelial-leukocyte adhesion molecules in human disease. *Annu. Rev. Med.,* **45,** 361–378.

Bothner-By,A.A., Stephens,R.L., Lee,J., Warren,C.D. and Jeanloz,R.W. (1984) Structure determination of a tetrasaccharide: transient nuclear Overhauser effects in the rotating frame. *J. Am. Chem. Soc.,* **106,** 811–813.

Cagas,P. and Bush,C.A. (1990) Determination of the conformation of Lewis blood group oligosaccharides by simulation of two-dimensional nuclear Overhauser data. *Biopolymers,* **30,** 1123–1138.

Cantor,C.R. and Schimmel,P.R. (1980) *Biophysical Chemistry. 1. The Conformation of Biological Macromolecules.* W. H. Freeman, New York.

Cavanagh,J., Fairbrother,W.J., Palmer,A.G.,Jr. and Skelton,N.J. (1996) *Protein NMR Spectroscopy: Principles and Practice.* Academic Press, San Diego.

Coteron,J.M., Singh,K., Asensio,J.L., Dominguez-Dalda,M., Fernandez-Mayoralas,A., Jimenez-Barbero,J., Martin-Lomas,M., Abad-Rodriguez,J. and Nieto-Sampedro,M. (1995) Oligosaccharides structurally related to E-selectin ligands are inhibitors of neural cell division: synthesis, conformational analysis and biological activity. *J. Org. Chem.,* **60,** 1502–1519.

Diacovo,T.G., Puri,K.D., Warnock,R.A., Springer,T.A. and von Adrian,U.H. (1996) Platelet-mediated lymphocyte delivery to high endothelial venules. *Science,* **273,** 252–255.

Ernst,R.R., Bodenhausen,G. and Wokaun,A. (1988) *Principles of Nuclear Magnetic Resonance in One and Two Dimensions.* Oxford University Press, New York.

Harlan,J.M. and Liu,D.Y. (1992) *Adhesion: Its Role in Inflammatory Disease.* W. H. Freeman, New York,

Hemmerich,S. and Rosen,S.D. (1994) 6′-Sulfated sialyl Lewis x is a major capping group of GlyCAM-1. *Biochemistry,* **33,** 4830–4835

Hemmerich,S., Leffler,H. and Rosen,S.D. (1995) Structure of the O-glycans in

GlyCAM-1, an endothelial-derived ligand for L-selectin. *J. Biol. Chem.*, **270,** 12035–12047.

Holmbeck,S.M.A., Petillo,P. and Lerner,L.E. (1994) The solution conformation of hyaluronan: a combined NMR and molecular dynamics study. *Biochemistry,* **33,** 14246–14255.

Homans,S.W. (1990) A molecular mechanics force field for the conformational analysis of oligosaccharides: comparison of theoretical and crystal structures of Man(alpha)1–3Man(beta)1–4)GlcNAc. *Biochemistry,* **29,** 9110–9118.

Ichikawa,Y., Lin,Y.-C., Dumas,D.P., Shen,G.-J., Garcia-Junceda,E., Williams, M.A., Bayer,R., Ketcham,C., Walker,L.E., *et al.* (1992) Chemical–enzymatic synthesis and conformational analysis of sialyl Lewis x and derivatives. *J. Am. Chem. Soc.,* **114,** 9283–9298.

Jeener,J., Meier,B.H., Bachmann,P. and Ernst,R.R. (1979) Investigation of exchange processes by two-dimensional NMR spectroscopy *J. Chem. Phys.,* **71,** 4546–4553.

Kogan,T.P., Dupre,B., Keller,K.M., Scott,I.L., Bui,H., Market,R.V., Beck,P.J., Voytus,J.A., Revelle,B.M., *et al.* (1995) Rational design and synthesis of small molecule, non-oligosaccharide selectin inhibitors: (alpha-D-mannopyranosyloxy)biphenyl-substituted carboxylic acids. *J. Med. Chem.,* **38,** 4976–4984.

Kogelberg,H. and Rutherford,T.J. (1994) Studies on the three-dimensional behaviour of the selectin ligands Lewis a and sulphated Lewis a using NMR spectroscopy and molecular dynamics simulations. *Glycobiology,* **4,** 49–57.

Kogelberg,H., Frenkiel,T.A., Homans,S.W., Lubineau,A. and Feizi,T. (1996) Conformational studies on the selectin and natural killer cell receptor ligands sulfo- and sialyl-lacto-N-fucopentanoses (SuLNFPII and SLNFPII) using NMR spectroscopy and molecular dynamics simulations. Comparisons with the nonacidic parent molecule LNFPII. *Biochemistry,* **35,** 1954–1964.

Kubes,P., Jutila,M. and Payne,D. (1995) Therapeutic potential of inhibiting leukocyte rolling in ischemia/reperfusion. *J. Clin. Invest.,* **95,** 2510–2519.

Lasky,L.A. (1995) Selectin–carbohydrate interactions and the initiation of the inflammatory immune response. *Annu. Rev. Biochem.,* **64,** 113–139.

Lasky,L.A., Singer,M.S., Dowbenko,D., Imai,Y., Henzel,W.J., Grimley,C., Fennie,C., Gillet,N., Watson,S.R. and Rosen,S.D. (1992) An endothelial ligand for L-selectin is a novel mucin-like molecule. *Cell,* **69,** 927–938.

Lemieux,R.U. (1996) How water provides the impetus for molecular recognition in aqueous solution. *Acc. Chem. Res.,* **29,** 373–380.

Lin,Y.-C., Hummel,C.W., Huang,D.-H., Ichikawa,Y., Nicolaou,K.C. and Wong,C.-H. (1992) Conformational studies of sialyl Lewis x in aqueous solution. *J. Am. Chem. Soc.,* **114,** 5452–5454.

Macura,S. and Ernst,R.R. (1980) Elucidation of cross relaxation in liquids by two-dimensional N.M.R. spectroscopy. *Mol. Phys.,* **41,** 95–117.

Macura,S., Huang,Y., Suter,D. and Ernst,R.R. (1981) Two-dimensional chemical exchange and cross-relaxation spectroscopy of coupled nuclear spins. *J. Mag. Res.,* **43,** 259–281.

Maly,P., Thall,A.D., Petryniak,B., Rogers,C.E., Smith,P.L., Marks,R.M., Kelly,R.J., Gersten,K.M., Cheng,G., Saunders,T.L., Camper,S.A., Camphausen,R.T., Sullivan,F.X., Isogai,Y., Hindsgaul,O., von Adrian,U.H. (1996) The a(1,3)fucosyltransferase Fuc-TVII controls leukocyte trafficking through an essential role in L:-, E-, and P-selectin ligand biosynthesis. *Cell,* **86,** 643.

Manning,D.D., Bertozzi,C.R., Pohl,N.L., Rosen,S.D. and Kiessling,L.L. (1995) Selectin–saccharide interactions: revealing structure–function relationships with chemical synthesis. *J. Organic Chem.,* **60,** 6254.

Manning,D.D., Bertozzi,C.R., Rosen,S.D. and Kiessling,L.L. (1996) Tin-mediated phophorylation: synthesis and selectin binding of a phospho Lewis a analog. *Tetrahedron Lett.,* **37,** 1953–1956.

McEver,R.P., Moore,K.L. and Cummings,R.D. (1995) Leukocyte trafficking mediated by selectin–carbohydrate interactions. *J. Biol. Chem.,* **270,** 11025–11028.

Mebius,R.R. and Watson,S.R. (1993) L- and E-selectin can recognize the same naturally occurring ligands on high endothelial venules. *J. Immunol.,* **151,** 3252–3260.

Miller,K.E., Mukhopadhyay,C., Cagas,P. and Bush,C.A. (1992) Solution structure of the Lewis x oligosaccharide determined by NMR spectroscopy and molecular dynamics simulations. *Biochemistry,* **31,** 6703–6709.

Mukhopadhyay,C. and Bush,C.A. (1991) Molecular dynamics simulation of lewis blood groups and related oligosaccharides. *Bioploymers,* **31,** 1737–1746.

Mukhopadhyay,C., Miller,K.E. and Bush,C.A. (1994) Conformation of the oligosaccharide receptor for E-selectin. *Biopolymers,* **34,** 19–21.

Nelson,R.M., Dolich,S., Aruffo,A., Cecconi,O. and Bevilacqua,M.P. (1993) Higher-affinity oligosaccharide ligands for E-selectin. *J. Clin. Invest.,* **91,** 1157–1166.

Neuhaus,D. and Williamson,M. (1989) The nuclear Overhauser effect in structural and conformational analysis. VCH, New York.

Polak,E. and Ribiere,G. (1969) Note sur la convergence de methods de directions conjuguees. *Rev. Franc. d' Info. Rech. Oper.,* **16-R1,** 35–43.

Rosen,S.D. and Bertozzi,C.R. (1994) The selectins and their ligands. *Curr. Opinion Cell Biol.,* **6,** 663–673.

Rutherford,T.J., Spackman,D.G., Simpson,P.J. and Homans,S.W. (1994) 5 nanosecond molecular dynamics and NMR study of conformational transitions in the sialyl-Lewis x antigen. *Glycobiology,* **4,** 59–68.

Sanders,W.J., Katsumoto,T.R., Bertozzi,C.R., Rosen,S.D. and Kiessling,L.L. (1996) L-Selectin–carbohydrate interactions: relevant modifications of the Lewis x trisaccharide. *Biochemistry,* **35,** 14862–14867.

Schleucher,J., Quant,J., Glaser,S. J. and Greisinger,C. (1995) A theorem relating cross relaxation and hartmann-hahn transfer in multiple-pulse sequences. optimal suppression of TOCSY transfer in ROESY *J. Mag. Res. Ser. A,* **112,** 144–151.

Senderowitz,H., Parish,C. and Still,W.C. (1996) Carbohydrates: united atom AMBER* parameterization of pyranoses and simulations yielding anomeric free energies. *J. Am. Chem. Soc.,* **118,** 2078–2086.

Senderowitz,H. and Still,W.C. (1997) A quantum mechanically-derived all-atom force field for pyranose oligosaccharides. AMBER* parameters and free energy simulations. *J. Organic Chem.,* in press.

Still,W.C., Tempczyk,A., Hawley,R.C. and Hendrickson,T. (1990) Semianalytical treatment of solvation for molecular mechanics and dynamics. *J. Am. Chem. Soc.,* **112,** 6127–6129.

Stoddart,J.J. (1971) *The Sterochemistry of Carbohydrates.* John Wiley, New York.

Tropp,J. (1980) Dipolar relaxation and nuclear Overhauser effects in nonrigid molecules: the effect of fluctuating internuclear distances. *J. Chem. Phys.,* **72,** 6035–6043.

Tvaroska,I., Hricovini,M. and Petrakova,E. (1989) An attempt to derive a new Karplus-type equation of vicinal proton-carbon coupling constants for C-O-C-H segments of bonded atoms. *Carbohydr. Res.,* **189,** 363–367.

van Halbeek,H. (1994) NMR Developments in structural studies of carbohydrates and their complexes. *Curr. Opinion Struct. Biol.,* **4,** 697–709.

Varki, A. (1994) Selectin ligands. *Proc. Natl. Acad. Sci. USA,* **91,** 7390–7397.

Wu,S.-H., Shimazaki,M., Lin,C.-C., Qiao,L., Moree,W.J., Weitz-Schmidt,G. and Wong,C.-H. (1996) Synthesis of fucopeptides as sialyl Lewis x mimetics. *Ang. Chem. Intl. Ed. Eng.,* **35,** 88–90.

Yuen,C.-T., Bezouska,K., O'Brien,J., Stoll,M., Lemoine,R., Lubineau,A., Kiso,M., Hasegawa,A., Bockovich,N. J., *et al.* (1994) Sulfated blood group Lewis a: a superior oligosaccharide ligand for human E-selectin. *J. Biol. Chem.,* **269,** 1595–1598.

Yuen,C.-T., Lawson,A.M., Chai,W., Larkin,M., Stoll,M.S., Stuart,A.C., Sullivan,F.X., Ahern,T.J. and Feizi,T. (1992) Novel sulfated ligands for the cell adhesion molecule E-selectin revealed by the neoglycolipid technology among O-linked oligosaccharides on an ovarian cystadenoma glycoprotein. *Biochemistry,* **31,** 9126–9131.

Received on August 6, 1996; revised on November 4, 1996; accepted on November 8, 1996